ANNUAL REVIEWS

Annual Review of Microbiology

Multiscale Dynamic Structuring of Bacterial Chromosomes

Virginia S. Lioy,[1] Ivan Junier,[2] and Frédéric Boccard[1]

[1]Université Paris-Saclay, CEA, CNRS, Institute for Integrative Biology of the Cell (I2BC), 91198 Gif-sur-Yvette, France; email: frederic.boccard@i2bc.paris-saclay.fr

[2]Université Grenoble Alpes, CNRS, TIMC-IMAG, 38000 Grenoble, France

Annu. Rev. Microbiol. 2021. 75:541–61

First published as a Review in Advance on August 3, 2021

The *Annual Review of Microbiology* is online at micro.annualreviews.org

https://doi.org/10.1146/annurev-micro-033021-113232

Keywords

bacteria, chromosome conformation, DNA supercoiling, condensins, nucleoid-associated proteins

Abstract

Since the nucleoid was isolated from bacteria in the 1970s, two fundamental questions emerged and are still in the spotlight: how bacteria organize their chromosomes to fit inside the cell and how nucleoid organization enables essential biological processes. During the last decades, knowledge of bacterial chromosome organization has advanced considerably, and today, such chromosomes are considered to be highly organized and dynamic structures that are shaped by multiple factors in a multiscale manner. Here we review not only the classical well-known factors involved in chromosome organization but also novel components that have recently been shown to dynamically shape the 3D structuring of the bacterial genome. We focus on the different functional elements that control short-range organization and describe how they collaborate in the establishment of the higher-order folding and disposition of the chromosome. Recent advances have opened new avenues for a deeper understanding of the principles and mechanisms of chromosome organization in bacteria.

Contents

1. INTRODUCTION

Bacterial DNA is efficiently compacted into the so-called nucleoid, a highly organized and dynamic cellular space containing the genetic material and its associated proteins, with both proteins and DNA playing a pivotal role. The observation of DNA loops and independent supercoiling domains in the *Escherichia coli* chromosome (100, 130), together with the observation by electron microscopy of chromosomes that resembled rosettes with supercoiled loops of DNA (53), has influenced our representation of chromosome organization in bacteria. For many years, the chromosome was represented as an entity with 50- to 100-kb independent modular domains. Development in this field was hindered by the difficulty of assessing chromosome structuring locally; most studies were performed with small replicons such as plasmids, viruses, or phages. Yet, remarkable progress has been achieved in the last 20 years, and new features of chromosome conformation and positioning have emerged.

Chromosome folding and compaction result from a combination of processes, including DNA supercoiling, the formation of bacterial chromatin composed of nucleoid-associated proteins (NAPs) bound to DNA, condensation by structural maintenance of chromosome (SMC) complexes, macromolecular crowding, out-of-equilibrium processes such as replication and transcription, and interaction with cellular structures. A number of reviews concerning several of these aspects have been published in recent years (4, 21, 118), including reviews focusing on bacterial epigenome regulation by DNA methylation or posttranslational modifications of NAPs (18, 92), on the interplay between bacterial chromatin and transcription (98), and on chromosome choreography during the cell cycle (22, 89). Here, we build upon both this literature and recent studies to focus on the control of the multiscale organization of chromosomes, with insights into the interplay between chromatin dynamics and chromosome folding.

Work performed in a limited number of bacterial models has underscored the multiscale structuring of the nucleoid with an interplay between the different levels. We discuss how DNA supercoiling is organized into stochastic 10-kb domains included in larger 30–400-kb chromosomal interaction domains (CIDs) delimited by long and highly expressed gene clusters. We also describe how bacterial chromatin composed of multiple proteins bound to DNA not only influences gene

expression but also modulates, together with bacterial SMC complexes, the folding and disposition of the chromosome in the cell. Finally, we disclose how dedicated systems define the formation of large ~1-Mb domains and contribute to global folding of the chromosome.

2. FACTORS INVOLVED IN CHROMOSOME STRUCTURING

Genomics and metagenomics approaches in the last decade have revealed the immense phylogenetic diversity of the bacterial kingdom (43, 75). Among other features, five genomic traits—genome size, GC content, the number of genes, the number of 16S rRNA genes, and the number of tRNA genes—are highly variable. By contrast, two genomic features that directly or indirectly impact chromosome structuring are well conserved. First, bacterial genetic information is generally carried on a circular chromosome with a single origin of replication, *oriC* (33), from which two replication forks proceed bidirectionally toward the opposite terminus region (referred to as Ter). Second, 90% of the genome corresponds to coding sequences [89 ± 3% of coding on average for 974 different bacterial genomes (75)]. Remarkably, a number of factors involved in chromosome structuring (e.g., topoisomerases, NAPs, SMC complexes) are widely conserved in bacteria, suggesting that various mechanisms have been maintained for this process across evolution.

2.1. DNA Topoisomerases

DNA supercoiling generated by complexes tracking along the DNA originates from the helical nature of DNA and from the difficulty of a moving complex in rotating around the double helix. Consequently, domains of negative and positive supercoiling are generated behind and ahead of the complex, respectively. The existence of the twin supercoiled domains (66) generated by transcription implies the involvement of topoisomerases in controlling topological perturbations.

Bacteria contain four different DNA topoisomerases—enzymes controlling the topological state of DNA by generating transient cuts in it and catalyzing the passage of DNA segments through these cuts before closing them. Topoisomerase (Topo) I and Topo III (type I topoisomerases) make transient DNA single-strand breaks, while DNA gyrase and Topo IV (type II topoisomerases) make DNA double-strand breaks. All four topoisomerases can relax DNA. In addition, DNA gyrase introduces supercoils into DNA. DNA gyrase and Topo IV cleave the DNA at multiple sites on the chromosome (93, 105). DNA gyrase replenishes downstream supercoil losses to maintain an equilibrium state ahead of complexes translocating along the DNA, while Topo I is thought to relax the excess of supercoiled DNA behind the transcription complex. Topo IV is responsible for the decatenation of entangled double-stranded DNA molecules (137), while Topo III may act as a decatenase at a single-strand gap at the replication fork (62).

2.2. Nucleoid-Associated Proteins

NAPs are highly abundant proteins [>3,000 copies per cell (1, 38, 95)] that play diverse roles as chromatin organizers, transcription factors, and more generally accessory partners involved in DNA transactions (23). At least ten families of abundant NAPs have been characterized in different bacterial species and may fulfill different activities for chromatin dynamics and nucleoid organization. Differences in the way NAPs are expressed and how they interact with DNA suggest that they may play different but complementary roles in nucleoid organization.

While it is tempting to associate NAP with specific functions on the basis of in vitro and in vivo ChIP-seq and HiC data, it is important to recall that, for example, inactivation of HU has no apparent defect in *Caulobacter crescentus*, while *E. coli* cells are strongly affected (2, 44). Furthermore, the effects on DNA contacts upon HU inactivation in these bacteria are opposite (61, 64). Therefore, interspecies extrapolations regarding different levels of nucleoid organization

and the role of NAPs should be considered with care. In this review, we focus on four types of proteins whose activity may be considered paradigms for NAP function in various bacteria: a dynamizer/bender that ensures chromatin dynamics (HU/IHF), a silencer (H-NS), a growth phase–dependent regulator (Fis), and a recently identified DNA topology controller (GapR).

2.2.1. HU/IHF. HU and IHF are closely related proteins that are conserved across the bacterial kingdom. Each protein is composed of two homologous subunits (HupA and HupB; IhfA and IhfB). In *E. coli*, while IHF exists as a heterodimer, HU can exist as either a homodimer or a heterodimer, depending on the growth stage. Both proteins show two different but overlapping modes of DNA binding: a nonspecific mode and a specific mode (**Figure 1*a***). In vitro, IHF binds specific sites with a defined sequence 1,000–10,000 times more tightly than nonspecific, chromosomal DNA (76, 121). IHF is used in two ways in *E. coli* cells: It is involved, on one hand, globally in nucleoid organization by binding in a sequence-independent manner to many DNA sites over a broad range of affinities and, on the other hand, locally as an architectural element in nucleoprotein complexes via its interaction with sequence-specific high-affinity DNA binding sites (76). HU shows similar differences in binding affinity between damaged or distorted DNA and nonspecific chromosomal DNA (83). That the DNA-binding parameters for HU are similar implies that HU also contributes significantly to nucleoid organization through nonspecific DNA binding. If one assumes that unbinding times, or equivalently off rates, are controlled by the strength of interactions inside the DNA-protein complex, the binding/unbinding of NAPs to/from nonspecific and specific sites would ensure chromatin dynamics (52).

2.2.2. H-NS. H-NS belongs to a protein family found in different α-, β-, and γ-proteobacteria, with five evolutionary protein clades of homologs that have been identified: H-NS, StpA, Hfp, HlpP, and HlpC (24, 32, 86). In addition to having roles as a transcription factor and in chromosomal structuring, H-NS prevents the expression of horizontally acquired AT-rich genes by polymerizing along extended DNA regions and exerting a xenogeneic silencing activity (**Figure 1*a***). In this process, H-NS, alone or in combination with its paralogs and modulators, forms nucleoprotein filaments responsible for the silencing of genes at different steps of the transcription process (14). As a consequence, H-NS can repress the expression of hundreds of gene targets by polymerizing from high-affinity nucleation sites along extended stretches of DNA (3, 15) and by forming higher-order structures that connect distant DNA loci through a so-called bridging mechanism (14). How these two processes are connected in vivo is not yet clear. Remarkably, researchers recently revealed that H-NS promotes sister chromatid cohesion in a specific region of the *Vibrio cholerae* chromosome (30).

2.2.3. Fis. Like IHF, Fis has been discovered to be a factor required for a site-specific recombination reaction, an inversion event (47, 54). Cellular levels of Fis vary considerably during the growth phase; it is one of the most abundant proteins during the early exponential phase, while its levels are very low in the stationary phase (6). It binds DNA both specifically to *fis* binding sites and nonspecifically (**Figure 1*a***). Like HU and H-NS, Fis regulates many genes both directly and indirectly through the regulation of other transcription factors (72). It is thought to play an important role in shaping nucleoid structure, as it bends DNA, organizes DNA loops and plectonemes (96, 101), and has been proposed to participate in the formation of topological domain barriers (39).

2.2.4. GapR. GapR is an essential 89-amino-acid-long protein conserved in α-proteobacteria and recently identified in *C. crescentus* to be required for growth, DNA replication, chromosome segregation, and cell division (2, 90, 106). GapR plays a critical role in replication elongation by resolving the superhelical stress that arises in front of the replication fork. GapR recognizes the

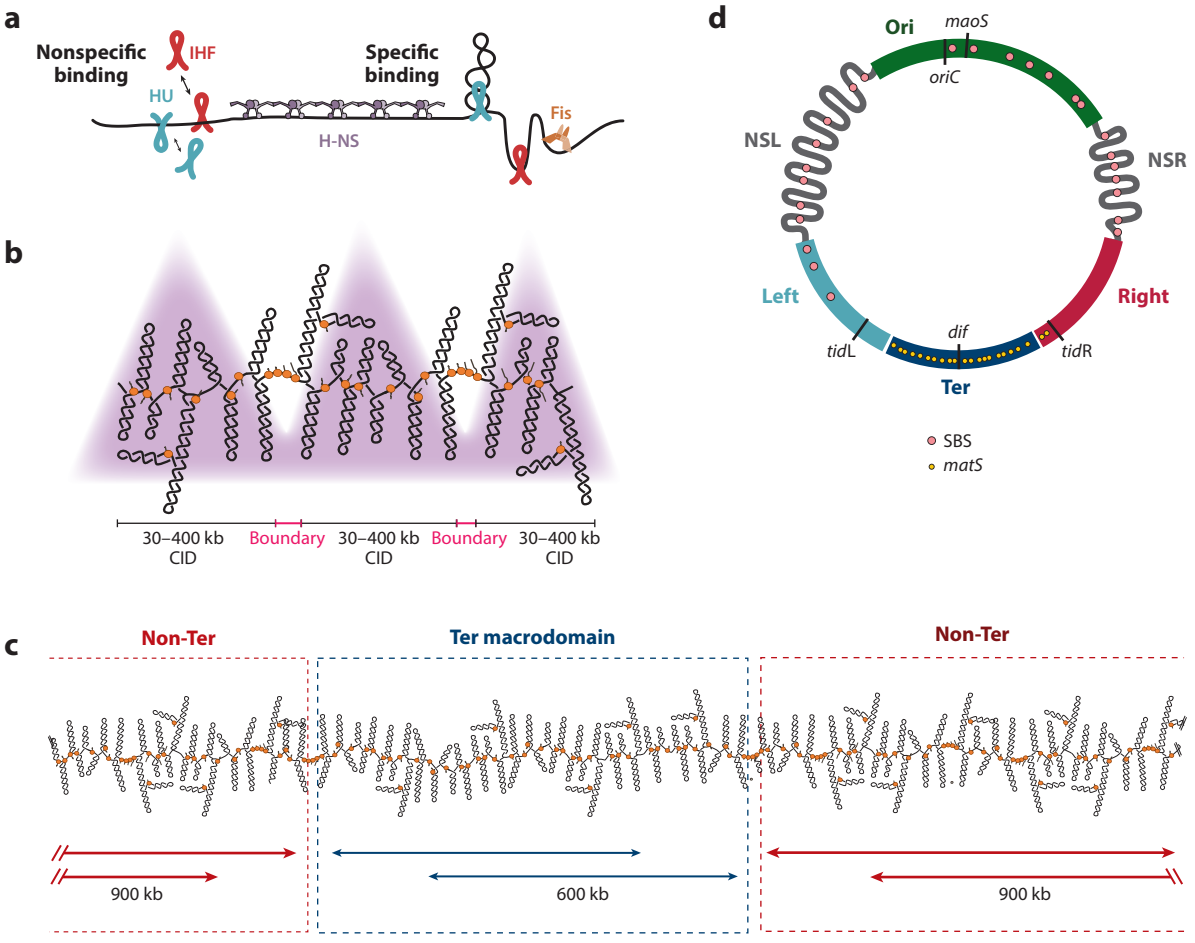

Figure 1

Multiscale organization of the *Escherichia coli* chromosome. (*a*) Four types of nucleoid-associated proteins contribute to chromatin formation and nucleoid organization through nonspecific, weak, and transitory interactions with the bulk chromosome (represented by *arrows* for HU and IHF) and through site-specific binding and DNA bending (HU, IHF, Fis). H-NS forms oligomers with DNA into an extended conformation; these oligomers silence target genes and prevent short-range contacts. For clarity, DNA supercoiled plectonemic structures were omitted. (*b*) Dynamics of supercoiled DNA. Slithering and branching of supercoiled DNA allow for long-distance (>100-kb) interactions. Depending on the amount of transcription, elongating RNA polymerase blocks supercoil diffusion at different levels. Long and highly expressed gene clusters compose chromosomal interaction domain (CID) boundaries, whereas transcription of less expressed genes generates short-lived diffusion barriers, defining the stochastic ~10-kb topological domains. For clarity, nucleoid-associated proteins bound to DNA were omitted. Orange circles represent transcribing RNA polymerase. (*c*) Long-distance interactions along the chromosome. In the Ter macrodomain, the presence of MatP prevents MukBEF activity, and contacts between loci are limited to 600 kb. Outside Ter, in the presence of MukBEF, contacts are extended to 900 kb. The Ter and flanking regions are shown. Thin blue and red arrows symbolize a lower and higher extent of interactions, respectively. (*d*) Chromosomal map of the four macrodomains (MDs) and the two nonstructured regions (NSL and NSR) (*wavy segments*). The determinants specifying properties to the *E. coli* chromosome are indicated: the unique *maoS* site near *oriC*; *matS* sites (*yellow circles*) in the 800-kb-long Ter domain; and two specific 12-bp sequences, *tid*R and *tid*L, located in the flanking left and right MDs. The difference between the nonstructured regions and the left and right lateral MDs depends on their position on the genetic map relative to *oriC*. SlmA binding sites (SBSs; *pink circles*) involved in nucleoid occlusion (108) are essentially absent from the Ter and right MDs.

shape of the DNA instead of specific sequences, with an average of 3,000 molecules present in a cell that assemble as dimers of dimers to clamp overtwisted DNA (38). It acts through the activation of Topo IV and DNA gyrase. GapR is proposed to work in regions of the genome where a high level of positive supercoils accumulates, i.e., in front of the replication fork as well as in regions where the transcription and replication machineries converge (38).

2.3. Bacterial Condensins

SMC proteins are highly conserved, nearly ubiquitously in living organisms. Eukaryotic organisms require multiple SMC proteins for several aspects of genome maintenance (134). In bacteria, SMC complexes also play critical roles in chromosome organization and segregation (see below). Three different SMC complexes (Smc-ScpAB, MukBEF, and MksBEF) sharing a similar overall structure have been identified and are termed bacterial condensins (35). Smc-ScpAB, the most conserved complex (the Smc protein is homologous to eukaryotic SMCs), is found in the majority of bacterial species. In some γ-proteobacteria, the Smc-ScpAB complex is replaced by MukBEF, the first SMC complex identified in a screen for mutants producing anucleate cells in *E. coli* (78). The MksBEF complex is distantly related to MukBEF and is scattered over the phylogenic tree (82). While some studies support the idea that Smc-ScpAB works as a dimer in *Bacillus subtilis* (129), ScpA subunits self-interact in *Corynebacterium glutamicum* (13), suggesting that the functional unit of Smc-ScpAB in *C. glutamicum* may be a dimer of dimers like MukBEF in *E. coli* (5, 88).

Bacterial SMC proteins comprise a nucleotide binding domain (or head) connected via an ~50-nm-long (1,000–1,500-amino-acid) antiparallel coiled coil to a hinge dimerization domain. The five-subunit Smc_2-$ScpAB_2$ complex forms an annular structure, which is thought to keep DNA double helices connected by coentrapment. The binding of both Smc heads by a single kleisin, ScpA, generates a tripartite ring, which associates (via ScpA) with two kite ScpB subunits. The Smc-ScpAB complex can transition from a rodlike conformation to an open ring upon ATP head engagement. Cycles of transition between the rod and open ring states would allow for DNA translocation, presumably by loop extrusion (117). The Smc (MukB and MksB) and kite (MukE and MksE) subunits of the MukBEF and MksBEF complexes are structurally similar to the canonical SMC subunits, except that MukB is longer (~65-nm) and the MksB coiled coil is shorter than the Smc subunits.

Smc-ScpAB essentiality varies across bacterial genera. Smc-ScpAB plays a role in chromosome management, together with the ParABS segregation system (see below). In *B. subtilis*, Smc-ScpAB is essential for chromosome segregation, even in the absence of ParABS (36, 127). By contrast, in *Pseudomonas aeruginosa* and *C. crescentus*, no important defects were observed for chromosome segregation upon inactivation of Smc-ScpAB (61, 65). While a rationale for the varying essentiality of Smc-ScpAB is still missing, MksBEF is required for chromosome segregation in *P. aeruginosa* mutants devoid of the ParABS system, and MukBEF, the *E. coli* condensin, can replace MksBEF (65).

2.4. Other Factors Involved in DNA Metabolism and Chromosome Management

Chromosome organization results not only from the interaction of structuring proteins with the DNA molecule but also from the targeting of numerous proteins involved in various aspects of DNA metabolism (reviewed in 109, 110). These systems include proteins interacting with specific motifs present in different copy numbers; in other words, bacterial genomes are imprinted by information required in *cis* to manage the chromosome during the cell cycle. Well-documented systems are involved in:

- replication initiation [the replication initiator DnaA and several DnaA box motifs in the chromosome replication origin (*oriC*) region (68)];

- segregation of the origin (Ori) region [the ParAB system and *parS* sites found in Ori regions (67)];
- general recombination [the RecBCD-like recombination system and Chi sites with a biased orientation along the replication arms (27, 56)];
- terminal segregation of the chromosome [the divisome-associated FtsK protein and KOPS motifs with a biased orientation along the replication arms (11, 63)];
- resolution of chromosome dimers [the site-specific Xer system and the unique *dif* site located opposite *oriC* (7, 55)];
- nucleoid occlusion, a process preventing cytokinetic ring assembly over the chromosome [the Noc/SlmA proteins and NBS/SBS motifs distributed over the genome, except in Ter regions (108, 133)];
- gene expression [DNA-bound transcriptional regulators and RNA polymerase bound to multiple promoters, as well as RNA polymerase during transcription elongation (98)]; and
- the formation of large chromosomal domains [the RacA or MatP proteins and their respective cognate binding *ram* (9) and *matS* (73) sites, which are found in a subregion of the genome].

3. METHODS TO INVESTIGATE CHROMOSOME STRUCTURING

During the past decades, a large number of methods have been developed to probe long-range chromosome organization in different bacterial models. Biophysical approaches [e.g., measurement of sedimentation coefficients upon DNase I treatment (130) and measurement of torsional tension by photobinding of trimethylpsoralen (100)], genetic approaches using site-specific DNA transaction systems (42, 114), and imaging approaches have been widely used (e.g., 29, 77, 125).

Moreover, genomic approaches have more recently yielded spectacular breakthroughs. Analyses of genomic loci bound by proteins have been performed using chromatin-immunoprecipitation (ChIP) followed by high-throughput sequencing of the immunoprecipitated DNA (ChIP-seq) (for example, 51, 85). Chromosome-conformation-capture (3C) methods disclose in particular the role of different structural factors in the control of chromosome folding. 3C technology is based on covalent cross-linking and proximity ligation of DNA fragments (**Figure 2*a***). The probability of contacts between distant loci is visualized on normalized contact maps (**Figure 2*a***). On every chromosome, the average intrachromosomal contact probability decreases monotonically, indicating polymer-like behavior in which the 3D distance between loci increases with increasing genomic distance. Two major methods have been used to compare 3C contact maps between wild-type and mutant cells (**Figure 2*d–j***). One can estimate the extent to which contacts are detected (65, 123) or compute a ratio map that recapitulates the variations in contacts between mutant and wild-type cells (64).

4. CHROMOSOME ORGANIZATION IN INFORMATIVE SPECIES

4.1. DNA Topology

In *E. coli*, DNA supercoiling exists roughly equally as interwound plectonemic DNA and as constrained DNA in alternative forms (12), likely by protein binding (120). In wild-type *E. coli* cells, transcription-induced negative supercoil waves were detected in vivo in the upstream region of a transcription unit and may affect regions as distant as 800 bp away (57, 87). Conversely, transcription-induced positive supercoils affect local supercoiling in downstream regions (87) at least several kilobases away from the site of origin (74). DNA gyrase catalytic targets behave as topological insulators by removing at least between 5 and 10 links per second (74).

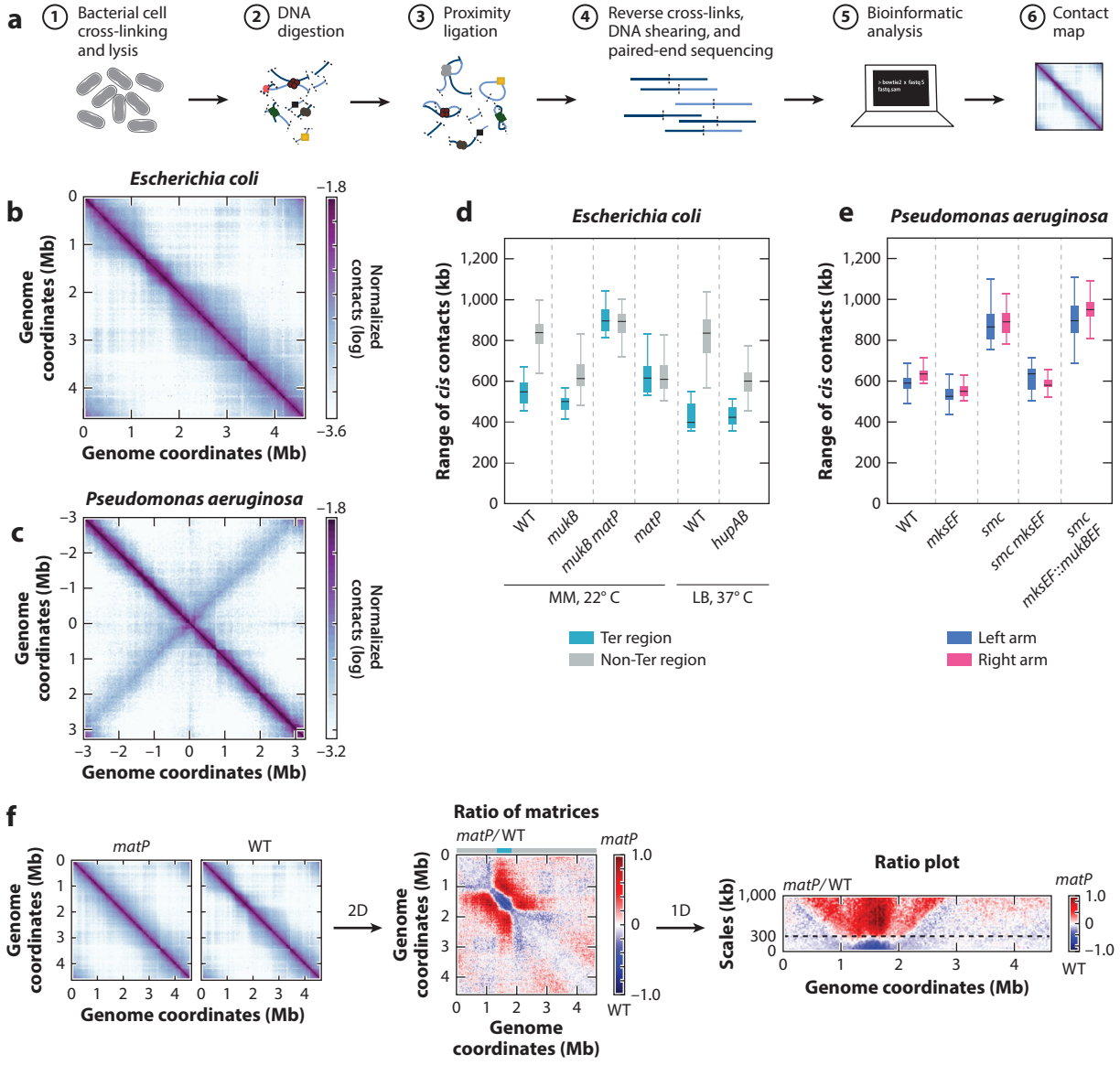

(*Caption appears on following page*)

Figure 2 (*Figure appears on preceding page*)

Long-range organization of chromosome revealed by the chromosome-conformation-capture (3C) method. (*a*) Schematized representation of the 3C method. In brief, (①) nucleoids are first fixed with formaldehyde. Then, cells are lysed, (②) cross-linked DNA is digested by a restriction enzyme, and (③) DNA fragments that are close in space are ligated together. (④) Finally, cross-linking is removed, DNA is purified, and DNA is prepared for paired-end sequencing (19). (⑤) After sequencing, reads are mapped to the reference genome and are assigned to the corresponding restriction fragments. (⑥) A raw matrix of contacts is built by representing the number of contacts between pairs of loci represented on the *x* and *y* axes. To remove any experimental bias, each row and column of the contact map is normalized to one (20, 46). Thus, normalized contact maps represent the relative frequency of contacts between distant chromosomal loci. Normalized contact maps are then visualized using heat maps, and each position reflects the probability of locus interactions. Regions with a higher probability of contacts are represented with a dark color (*dark purple*), whereas regions with a lower probability of contacts are represented in white. (*b*) Normalized contact map obtained for *Escherichia coli* MG1655 wild-type (WT) cells. (*c*) Normalized contact maps obtained for the *Pseudomonas aeruginosa* WT strain. (*d*) Quantification of the extent of *cis* contacts for *E. coli* contact maps of the WT strain and *mukB*, *mukB matP*, and *matP* mutants grown in minimal medium (MM) at 22°C and of the WT strain and the *hupAB* mutant grown in rich LB medium at 37°C. (*e*) Quantification of the range of *cis* contacts of *P. aeruginosa* chromosomal loci in WT and in *mksEF*, *smc*, *smc mksEF*, and *smc mksEF*::*mukBEF* cells. (*f*) Ratio of normalized contact maps of exponentially growing *matP* versus WT cells. A blue signal and a red signal denote a decrease and an increase, respectively, in contacts in one condition relative to the other. No change is represented by a white signal. Ratio plots recapitulate the variations in contacts between two conditions made by each bin with its neighboring bins, indiscriminately of their left or right positions. The *x* axis indicates the position of the bin along the genome. The *y* axis indicates the distance from the bin. (*g–j*) Ratio plots of the mutant and WT contact signals for each 5-kb bin (*g*,*i*) or 10-kb bin (*h*,*j*) along the chromosome. The mutant is identified above the plot. Panels *b*, *f*, *g*, and *i* adapted from Reference 64. Panels *c*, *d*, and *e* adapted from Reference 65. Panels *h* and *j* produced from data in Reference 65.

To investigate the supercoil structure and dynamics of the chromosome in *Salmonella enterica serovar* Typhimurium, a site-specific recombination system of γδ transposons that reports the topological state of the chromosome revealed that *res* sites separated by more than 90 kb may become tangled together within a supercoiled synapse (42, 102). In other words, slithering and branching of supercoiled DNA allow distant loci to interact within a plectonemic synapse. By using short-lived γδ recombinases (103) to reveal determinants that may modulate supercoiling slithering, barriers hampering supercoiling slithering would be present on average every 13 kb. Remarkably, elongating RNA polymerase was subsequently shown to block supercoil diffusion (91, 94), providing a simple rationale involving gene transcription for the stochastic nature of the barriers of topological domains at the 10-kb scale.

The recent development of 3C-seq/HiC techniques (**Figure 2*a***) has revealed that the chromosome in different bacteria is segmented into CIDs, in which DNA contacts occur readily; these CIDs range in length from 30 to 400 kb (61). Remarkably, these domains very often display long and highly expressed genes at their boundaries, even though not all highly transcribed genes are associated with boundaries. Interestingly, in *C. crescentus* the above recombination assays confirmed that active transcription blocks supercoiling diffusion but also revealed that not all supercoil diffusion barriers are CID boundaries (60). Rather, only long and highly expressed genes produce a CID boundary, indicating that both transcription rate and transcript length drive the formation of domain boundaries. Altogether, these findings suggest a scenario in which the bacterial genome is segmented into 30–400-kb-long domains composed of ∼10-kb-long branched plectonemes and flanked by boundaries generated by highly transcribed long genes or clusters of genes (60) (**Figure 1*b***). Significantly, long-range contacts are detected across CID boundaries, indicating either that the existence of another process or other processes allows for contacts between flanking regions independently of the slithering of supercoiled DNA or that the expression of long and highly expressed genes is not absolute among cells.

DNA supercoiling in vivo does not seem to be affected by the absence of the NAPs HU, IHF, or StpA, as revealed by a genetic screen in *E. coli* (39). The situation for HU is nonetheless controversial, as recent studies suggest that HU may establish, in the stationary phase, a higher level of (negative) supercoiling near Ter (59). Concerning H-NS and Fis, several works consistently lead to

a scenario in which these two NAPs are involved in the maintenance of the negative supercoiling of the *E. coli* chromosome (39, 97). The underlying mechanism remains unclear (see below).

4.2. Chromatin Dynamics

ChIP-seq and 3C techniques have been used to explore the contribution of NAPs and SMC complexes to chromatin organization and nucleoid organization. Comparison between contact maps from wild types and mutants revealed how NAPs and SMC complexes play different roles in chromatin organization.

Genome-wide, high-resolution investigation of HU binding to the *E. coli* chromosome (85) has confirmed that HU binds uniformly on the chromosome, with a preference for AT-rich sequences (58). 3C approaches revealed a reduction in long-range contacts (i.e., >300 kb) in the *hupAB* mutant, concomitant with an increase in contacts up to 300 kb (**Figure 2*d***). Remarkably, this increase in contacts is similar to that observed in MukBEF mutants, with the *E. coli* condensin promoting long-range contacts in *E. coli* (see below). Altogether, these results indicate that HU is an important component of the chromatin organization of *E. coli* and is required for optimal MukBEF activity in promoting DNA contacts up to the megabase range (64). Within such HU-MukBEF cooperation, HU is likely to act as a cofactor of the DNA management process by MukBEF, possibly by generating DNA properties that are essential for optimal MukBEF activity (64). This assumption is further supported by the analysis of HU molecules that were shown by single-molecule tracking to decondense the nucleoid through nonspecific, weak, and transitory interactions with the bulk chromosome (10).

Genome-scale investigation of H-NS binding to the *E. coli* chromosome by ChIP-seq has confirmed that H-NS binds in vivo to long tracts of DNA of average and maximal lengths of ~1,700 bp and ~10 kb, respectively, and that the length of binding regions is correlated with the intensity of transcriptional repression (51, 120). The possible role of H-NS in chromosome organization has also been investigated using 3C techniques by comparing contact maps obtained in wild-type and *h-ns* mutant cells (64). Results show a significant enrichment, for the mutant, in short-range contacts associated with H-NS binding regions. This finding implies that H-NS-bound loci are prevented from interacting with their neighboring loci. No evidence for DNA bridging between distant DNA loci or for the proposed H-NS-promoted juxtaposition of H-NS-regulated operons, as proposed previously (122), was revealed by genomic 3C approaches. Rather, ChIP-seq and 3C-seq approaches suggest that the main activity of H-NS in vivo relies on its ability to form long oligomers with DNA into an extended conformation that silences target genes and prevents short-range contacts.

Genome-scale investigation of Fis binding by ChIP-seq in *E. coli* indicates that Fis is associated with the differential expression of approximately 500 genes, i.e., only 40% of the genes that are bound by Fis (51). The 3C contact map for *fis* mutant cells shows that the overall chromosome conformation remains globally conserved relative to the wild type (64). In the absence of Fis, an enrichment of short-range contacts (<100 kb) and a decrease in contacts above 100–400 kb can nevertheless be observed from 3C data, especially in the Ter region. In contrast to the case for H-NS, changes in contact properties do not correlate with the density of Fis binding sites, leaving the mechanism of action of Fis an open question.

Investigation of the effect of MukBEF on chromatin organization by 3C methods revealed that MukBEF inactivation has the same effect as HU inactivation; ratio plots showed a reduction in long-range (>~300-kb) contacts and an increase in contacts up to 300 kb (64). This reduction of contacts above 300 kb obtained from ratio plots is concomitant with a change in the extent of long-range contacts from ~900 to ~600 kb (65) (**Figure 2*d***). Similar parameters are also observed in the *E. coli* Ter domain, where the presence of MatP prevents MukBEF activity (**Figure 2*d***; see below).

Remarkably, similar differentials of contacts around 300 kb were observed in *P. aeruginosa smc* mutants in the presence of MksBEF or in *P. aeruginosa* expressing the *E. coli mukBEF* genes (65) (**Figure 2*e***). These results lead us to postulate that, in these distant bacteria, the chromatin is constituted by a common basal fold. Interactions are modulated by the activity of condensins like MukBEF/MksBEF and of HU. Further studies will be necessary to characterize the parameters that modulate DNA contacts in the bacterial chromatin, to assess the putative contribution of factors such as DNA supercoiling and NAPs to these properties, and to reveal how MukBEF/MksBEF condensins promote long-range contacts along the chromosome (**Figure 3*b***). In contrast to the cases of MukBEF and MksBEF, Smc-ScpAB has no effect on long-range contacts within chromosome arms in *P. aeruginosa* (65).

4.3. Chromosomal Domains

Higher-order levels of organization of bacterial chromosomes have recently been described, disclosing large chromosomal regions organized into so-called macrodomains (MDs).

4.3.1. Long-range organization of the *Escherichia coli* chromosome. In *E. coli*, large regions (600 kb–1 Mb in size) have been identified using different approaches. Using FISH, MDs centered at the Ori and Ter regions were identified first in *E. coli* by Niki and colleagues (79) as large regions in which loci show similar localization patterns. A genetic system that revealed DNA collisions between spatially close loci was used to disclose MDs as long genomic domains inside which DNA collisions occurred preferentially, while DNA interactions in between were highly restricted; Ori, Ter, two additional intermediary MDs (left and right), and two nonstructured regions were identified (114) (**Figure 1*d***). This organization was then directly confirmed by fluorescence microscopy since the structuring in MDs and nonstructured regions influences the dynamics and the segregation of the chromosome (29).

The Ori domain depends on the MaoP/*maoS* system for constraining DNA mobility in this region and for limiting long-distance DNA collisions with other regions of the chromosome (115). *maoS* acts in *cis* as a unique organizing center from which MD properties spread to the entire MD. MaoP belongs to a group of proteins (including SeqA, MukBEF, and MatP); these proteins are conserved in the *Enterobacteria*, are involved in the control of DNA maintenance and chromosome conformation, and coevolved with Dam methylase (16). The underlying molecular mechanism remains to be characterized.

Genetic readout based on long-distance collisions showed that the replication cycle plays a prominent role in determining the localization of right and left MDs (25). The difference between the nonstructured regions and the right and left lateral MDs is based on their positions on the genetic map relative to *oriC*. Regardless of DNA sequence, the chromosome regions closest to *oriC* are always nonstructured, while the regions further away behave as MDs.

4.3.2. Function and anatomy of the *Escherichia coli* terminus domain. Organization of the Ter region into an MD depends on the presence of 23 *matS* sites in the 800-kb-long domain that constitute the main target of the protein MatP (73) (**Figure 1*d***). With the 3C method, the Ter MD is detected in the contact map as a constrained domain with limited long-range contacts (64) (**Figure 2*b***).

Several activities have been associated with the *E. coli* Ter MD. The interaction of MatP with the protein ZapB associated with the divisome promotes the anchoring of Ter at mid-cell (28). Other specificities of Ter originate from the inhibition of MukBEF activity by MatP independently of the interaction with ZapB (64, 80). Unlike Smc-ScpAB complexes that align chromosome arms in several bacteria (see below), MukBEF gives rise to long-range *cis* contacts within replication arms.

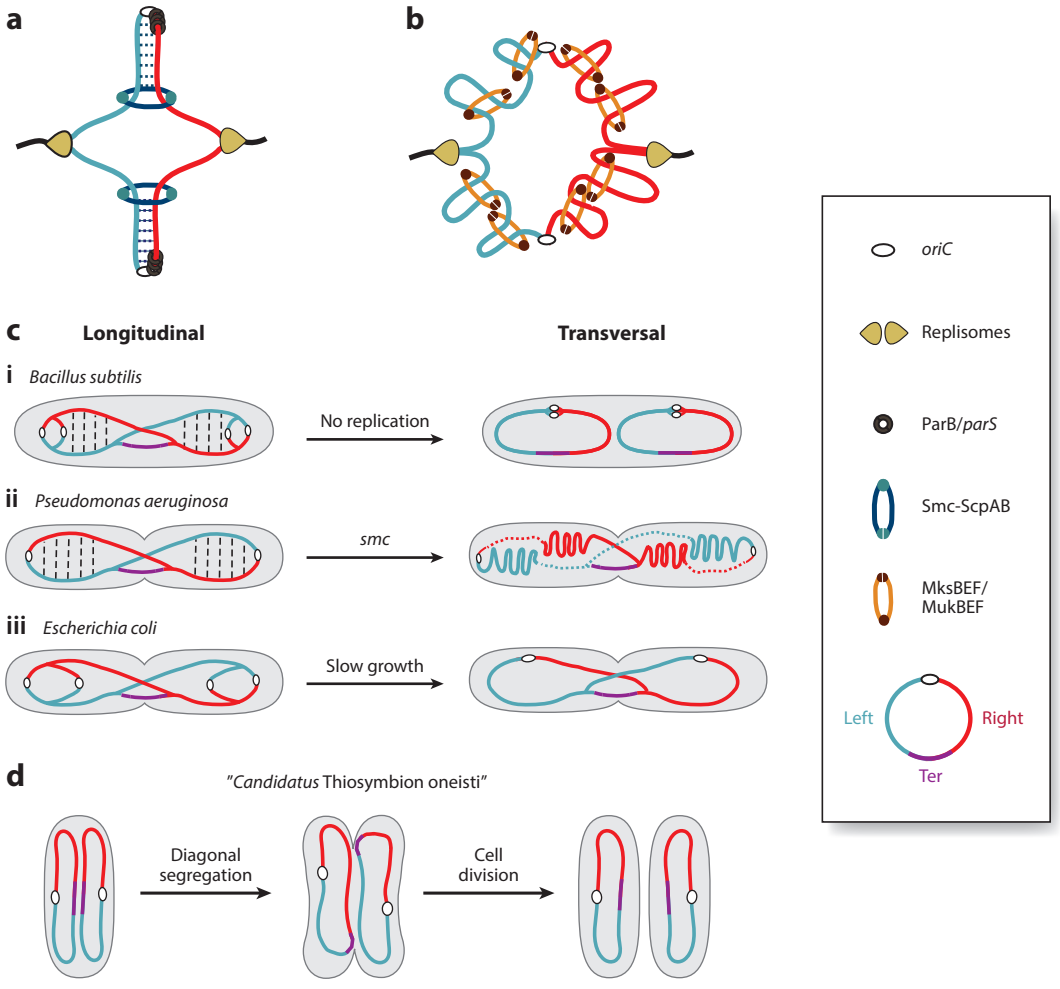

Figure 3

Model of bacterial condensins' activities and overall chromosome disposition. (*a*) Schematized representation of replication arm alignment by Smc-ScpAB in *Pseudomonas aeruginosa*. The two replisomes replicate from *oriC* at the left and right arms of the chromosome. Translocation of Smc-ScpAB from *parS* sites promotes the juxtaposition of chromosome arms. (*b*) Schematized representation of long-range contacts generated by MksBEF in *P. aeruginosa* (in the absence of Smc-ScpAB) or by MukBEF in *Escherichia coli*. These bacterial condensins produce long-range contacts within replication arms, presumably in a progressive manner and following the replication process, as evidenced by the activity of MksBEF in *P. aeruginosa*. (*c*) Chromosome disposition in a number of bacteria at different stages of the cell cycle or in different conditions. (*i*) *Bacillus subtilis* chromosome arrangement oscillates between a longitudinal disposition allowing for chromosomal arm contacts during the replication cycle and a transversal disposition after replication. (*ii*) In *P. aeruginosa*, the ParABS system drives the segregation of origin (Ori) regions to 20–80% of the cell, and translocation of Smc-ScpAB from *parS* sites promotes the juxtaposition of chromosome arms and a longitudinal organization of the chromosome (65). The position of a *parS* site(s) near *oriC* determines the orientation of the chromosome in the cell. In the absence of Smc-ScpAB, the juxtaposition of chromosome arms and the longitudinal disposition of the chromosome are lost, with the two arms of the chromosome in separate halves of the cell (65). (*iii*) In *E. coli*, in fast growth conditions, the chromosome adopts a longitudinal *ori-ter* (where *ter* denotes Terminus) orientation, with no contacts between the two arms. In slow growth conditions, the chromosome shows a transversal organization, with the left and right arms segregated to the left and right halves of the cell, respectively. (*d*) Chromosome disposition in the rod-shaped symbiont "*Candidatus* Thiosymbion oneisti." Division occurs longitudinally, sister *ori* segregate diagonally prior to septation onset, and the two *ter* regions migrate to mid-cell concomitantly with septation progression. Panel *a* and subpanel *ii* of panel *c* adapted from Reference 65.

By preventing MukBEF activity in Ter (64, 80), MatP limits the range of long-range contacts to 600 kb in this region (**Figure 2*d*,*g*,*i***). The interplay of MatP with MukBEF associated with Topo IV may ensure timely chromosome unlinking and segregation (80).

Structural and functional analysis of MatP and in vitro microscopic observations of MatP-dependent loop formation of DNA molecules carrying multiple *matS* sites suggested that Ter organization is mediated by the bridging of distant *matS* sites (26). However, 3C analyses did not unveil any discrete in vivo intrachromosomal *matS-matS* contacts (64). Furthermore, in the presence of MatP, the chromosome and plasmids carrying *matS* sites also required ZapB to be brought together. The same plasmids in the presence of ZapB contacted Ter, but no discrete *matS-matS* interactions could be identified. Together, these results show that in vivo MatP does not promote DNA bridges between *matS* sites either in *cis* or in *trans*. These results also reveal that MatP-ZapB interactions at the divisome are responsible for the clustering of distinct DNA molecules carrying *matS* sites (64). A constraining process that reduces DNA mobility and delays locus segregation (107) is regulated during the cell cycle and occurs only when the Ter MD is associated with the division machinery at mid-cell. A site-specific system composed of (*a*) two specific 12-bp sequences (*tid*R and *tid*L) located in the flanking left and right MDs (**Figure 1*d***) and (*b*) a newly identified protein designated as YfbV and conserved with MatP through evolution restricts this process to the Ter region (107).

So, how does MatP organize Ter in vivo? On the one hand, early experiments supported a scenario of Ter condensation by MatP-induced clustering of *matS* sites in a confined space. Such research includes the visualization of MatP foci and Ter tags by epifluorescence (28, 73) and the visualization of clustered MatP molecules by super-resolution microscopy (17). On the other hand, other results suggest that MatP creates an extended and thin Ter domain (see below) that can be spread over distant regions of the same cell (69, 125, 131). As genetic analyses of collisions within Ter or 3C data (64) do not allow for discrimination between these two possibilities, further experiments are required to determine precisely how MatP affects the organization of this region.

4.3.3. Large domains in other bacteria. Large domains have also been reported in other species, e.g., *B. subtilis* and *C. crescentus*, and are suspected in other genera.

In *B. subtilis*, the existence of different types of domains in the Ori region has been described at two developmental stages of the bacteria. First, in cells growing vegetatively, a 3C contact map disclosed a well-defined, ~1.4-Mb substructure composed of a pair of nested hairpin structures involving the Smc-ScpAB complex and the ParBS system (71). The Ori domain appears as a dynamic structure that is folded or unfolded to regulate chromosome replication. Interestingly, single-cell super-resolution microscopy revealed the presence of high-density chromosomal regions (HDRs), a new nucleoid substructural feature whose nature remains to be characterized. HDRs may correlate with the grouping of multiple CIDs, since the mean HDR size is higher than the mean CID size in *B. subtilis* (71). The average number of HDRs in wild-type cells varies from 7.8 to 15, depending on the cell cycle, and this number is considerably higher in *parB* or *smc* mutants, consistent with an increase in distance between the two replication arms in these mutants. In addition, only HDRs found in the Ori region display conserved subcellular localization, with a choreography that overlaps to a large extent with the segregation of ParB-gfp or a single *parS* site. Second, in cells that have begun to sporulate, the developmental protein RacA binds 25 *ram* sites present in an ~600-kb region near Ori. By promoting the anchoring of this region to the cell poles, RacA ensures the proper positioning of the Ori region for chromosome segregation during sporulation (9).

A system analogous to MatP-ZapB and connecting the chromosome Ter region with the divisome was recently identified in *C. crescentus* (81). The spatial connection is mediated by ZapT, a novel divisome-associated protein that interacts with Ter and associates with two proteins of

the division apparatus: ZapA and ZauP. The conservation of ZapT in proteobacteria and MatP in enterobacteria highlights the importance of a molecular bridge between Ter and the divisome coordinating chromosome segregation and cell division.

The functional implications of MDs remain to be better understood. An interesting aspect comes from the physical properties of a system in which molecular disorder, as provided either by nonstructured chromosomal regions or by the cytoplasm, and large condensed structures like MDs coexist. This coexistence necessarily leads to depletion forces (reviewed in 48), which strongly affect the cellular organization of chromosomes (99). In this regard, simulations indicated that the specific MD organization in *E. coli* strongly and specifically enhances entropic forces (50), which have been proposed to be responsible for driving the segregation of replicated nucleoids in bacteria lacking a ParABS-like active process (49).

4.4. Global Folding of the Chromosome

The disposition of the chromosome within the cell differs between bacterial species, and these differences may originate from the activity of different factors involved in chromosomal folding and segregation. Two main dispositions, longitudinal and transversal, have been described in the past 15 years, although variations on these organizations or other arrangements have been described (**Figure 3*c***), in agreement with the wide diversity of bacterial chromosome organizations unveiled by a metagenomics extension of 3C (70). In *C. crescentus*, *P. aeruginosa*, *Myxococcus xanthus*, and *Mycoplasma pneumoniae*, the chromosome is longitudinally disposed inside the cell, with the two replication arms aligned along the long axis of the cell (40, 61, 112, 113, 116, 119). In *E. coli*, the two chromosome arms locate to separate cell halves in a transversal disposition (77, 125). In *B. subtilis*, chromosome arrangement oscillates between the longitudinal and transversal organizations (126). In "*Candidatus* Thiosymbion oneisti," a rod-shaped symbiont that divides longitudinally, the chromosome displays a transverse organization, and the Ori regions segregate diagonally (128) (**Figure 3*d***).

In bacteria with a longitudinal disposition of the chromosome, the positioning and alignment of the chromosome arms result from the activity of the segregation system ParABS and of Smc-ScpAB (**Figure 3*a***). Smc-ScpAB is recruited to the Ori region by ParB bound to its cognate *parS* site and mediates chromosomal interarm contacts in *B. subtilis*, *C. crescentus*, *C. glutamicum*, and *P. aeruginosa* (13, 61, 65, 71, 124). 3C was used to show that, in *B. subtilis* and *C. crescentus*, SMC translocation from *parS* coincides with the zipping up of chromosome arms proceeding all the way to the Ter region (111, 123), presumably by a DNA loop extrusion mechanism (for a review, see 41). In *P. aeruginosa*, inactivation of Smc-ScpAB nevertheless affects the longitudinal arrangement of the chromosome with, remarkably enough, chromosome arms that tend to occupy separate halves of the cell, even when the *parS* region is properly positioned at the poles of the cell (65). These results indicate that in *P. aeruginosa*, chromosome arms spontaneously arrange in opposite cell halves (**Figure 3*c***).

In *E. coli*, the disposition and the choreography of the chromosome vary with growth rate (8). Numerous studies have revealed, during slow growth conditions, a transversal disposition of the chromosome (77, 125), with the position of loci recapitulating the genetic map and loci present in MDs showing a similar pattern (29, 79). In fast growth conditions, chromosome disposition shifts to a longitudinal *ori-ter* orientation (135), even though genetic and 3C approaches disclosed the absence of contacts between the two arms (64, 114). The processes controlling the global folding of the *E. coli* chromosome are not fully understood. One assumption is that MukBEF acts in concert with Topo IV to direct the normal positioning of sister Ori regions after their replication and during their segregation (136).

4.5. Organizing the Chromosome into the Nucleoid

Remarkably, in diverse bacteria, nucleoid size strongly correlates with cell size, independently of changes in DNA amount and across various nutrient conditions. Moreover, different biophysical cytoplasmic properties, including ribosome mobility and localization, are associated with different nucleocytoplasmic ratios (34).

In *E. coli* cells, fluorescence microscopy experiments revealed that nucleoids are arranged by radial confinement as helical ellipsoids and present highly dynamic loci governed by extension and shortening of nucleoid-longitudinal density waves (31). Another study showed that large (~140-kb) segments excised from the chromosome are evicted from the nucleoid and are positioned at the edge of the nucleoid (84), confirming the radial confinement of the nucleoid. By inhibiting cell division and analyzing nucleoid size and position, Dekker and colleagues (132) disclosed that longitudinal confinement sets the size and position of the nucleoid, with single nucleoids residing robustly at mid-cell while two nucleoids self-organize at the one-quarter and three-quarter positions. In *E. coli* cells that artificially widen (131), the chromosome possesses a torus topology, with a lower density near the origin of replication and an ultrathin flexible string of DNA at the Ter region. The torus appears heterogeneous, with bloblike megabase-size domains that show major dynamic rearrangements, splitting and merging at a minute timescale. MatP is crucial for the formation of prominent domain boundaries at both the *dif* and *oriC* regions (131). In conditions of increased chromosome occupancy of MukBEF, the chromosome is proposed to be organized as a series of loops around a thin MukBEF axial core, except in Ter, where MatP displaces MukBEF (69).

5. CONCLUSION AND PERSPECTIVES

Recent new developments in imaging and genomic approaches have improved our understanding of bacterial chromatin and chromosome organization. Bacterial chromosome organization relies on several structuring processes operating at different scales. Bacterial genomes are imprinted by *cis* information required for DNA metabolism and chromosome management. Transcription modulates the dynamics of DNA supercoiling, and long and highly expressed gene clusters limit interactions between flanking regions. Highly abundant NAPs play complementary roles in bacterial chromatin. Three types of bacterial condensins manage chromosome differently. NAPs, condensins, and topoisomerases collaborate to control the dynamic folding of the chromosome.

Posttranslational modifications in NAPs have been identified in bacteria (18), and the extent of epigenetic control in chromosome function remains to be explored. Additionally, structures that involve liquid-liquid phase separation (45) and that play a fundamental role in the compartmentalization of the eukaryotic nucleus (104) are also present in bacteria, as shown for the segregosome complex (37). It will thus be important to assess the use and impact of liquid-liquid phase separation in the organization of bacterial chromatin.

Several aspects of processes involved in higher-order nucleoid organization and in the faithful segregation of replicated chromosomes remain to be unraveled. Novel experimental tools and methods and realistic multiscale biophysical modeling of the bacterial chromosome appear to be necessary to properly apprehend how interactions at the molecular scale assemble to control processes at the cellular scale.

DISCLOSURE STATEMENT

The authors are not aware of any affiliations, memberships, funding, or financial holdings that might be perceived as affecting the objectivity of this review.

ACKNOWLEDGMENTS

We thank members of the F.B. and I.J. laboratories for fruitful discussions. We apologize to many colleagues for not being able to cite their work due to space constraints. Part of the research performed in F.B.'s lab has been supported by the Association pour la Recherche sur le Cancer.

LITERATURE CITED

1. Ali Azam T, Iwata A, Nishimura A, Ueda S, Ishihama A. 1999. Growth phase–dependent variation in protein composition of the *Escherichia coli* nucleoid. *J. Bacteriol.* 181(20):6361–70
2. Arias-Cartin R, Dobihal GS, Campos M, Surovtsev IV, Parry B, Jacobs-Wagner C. 2017. Replication fork passage drives asymmetric dynamics of a critical nucleoid-associated protein in *Caulobacter*. *EMBO J.* 36(3):301–18
3. Arold ST, Leonard PG, Parkinson GN, Ladbury JE. 2010. H-NS forms a superhelical protein scaffold for DNA condensation. *PNAS* 107(36):15728–32
4. Badrinarayanan A, Le TB, Laub MT. 2015. Bacterial chromosome organization and segregation. *Annu. Rev. Cell Dev. Biol.* 31:171–99
5. Badrinarayanan A, Reyes-Lamothe R, Uphoff S, Leake MC, Sherratt DJ. 2012. In vivo architecture and action of bacterial structural maintenance of chromosome proteins. *Science* 338(6106):528–31
6. Ball CA, Osuna R, Ferguson KC, Johnson RC. 1992. Dramatic changes in Fis levels upon nutrient upshift in *Escherichia coli*. *J. Bacteriol.* 174(24):8043–56
7. Barre F-X, Søballe B, Michel B, Aroyo M, Robertson M, Sherratt D. 2001. Circles: the replication-recombination-chromosome segregation connection. *PNAS* 98(15):8189–95
8. Bates D, Kleckner N. 2005. Chromosome and replisome dynamics in *E. coli*: Loss of sister cohesion triggers global chromosome movement and mediates chromosome segregation. *Cell* 121(6):899–911
9. Ben-Yehuda S, Fujita M, Liu XS, Gorbatyuk B, Skoko D, et al. 2005. Defining a centromere-like element in *Bacillus subtilis* by identifying the binding sites for the chromosome-anchoring protein RacA. *Mol. Cell* 17(6):773–82
10. Bettridge K, Verma S, Weng X, Adhya S, Xiao J. 2020. Single-molecule tracking reveals that the nucleoid-associated protein HU plays a dual role in maintaining proper nucleoid volume through differential interactions with chromosomal DNA. *Mol. Microbiol.* 115:12–27
11. Bigot S, Saleh OA, Lesterlin C, Pages C, El Karoui M, et al. 2005. KOPS: DNA motifs that control *E. coli* chromosome segregation by orienting the FtsK translocase. *EMBO J.* 24(21):3770–80
12. Bliska JB, Cozzarelli NR. 1987. Use of site-specific recombination as a probe of DNA structure and metabolism in vivo. *J Mol. Biol.* 194(2):205–18
13. Böhm K, Giacomelli G, Schmidt A, Imhof A, Koszul R, et al. 2020. Chromosome organization by a conserved condensin-ParB system in the actinobacterium *Corynebacterium glutamicum*. *Nat. Commun.* 11(1):1485
14. Boudreau BA, Hron DR, Qin L, van der Valk RA, Kotlajich MV, et al. 2018. StpA and Hha stimulate pausing by RNA polymerase by promoting DNA-DNA bridging of H-NS filaments. *Nucleic Acids Res.* 46(11):5525–46
15. Bouffartigues E, Buckle M, Badaut C, Travers A, Rimsky S. 2007. H-NS cooperative binding to high-affinity sites in a regulatory element results in transcriptional silencing. *Nat. Struct. Mol. Biol.* 14(5):441–48
16. Brézellec P, Hoebeke M, Hiet MS, Pasek S, Ferat JL. 2006. DomainSieve: a protein domain–based screen that led to the identification of dam-associated genes with potential link to DNA maintenance. *Bioinformatics* 22(16):1935–41
17. Buss J, Coltharp C, Shtengel G, Yang X, Hess H, Xiao J. 2015. A multi-layered protein network stabilizes the *Escherichia coli* FtsZ-ring and modulates constriction dynamics. *PLOS Genet.* 11(4):e1005128
18. Carabetta VJ. 2021. Addressing the possibility of a histone-like code in bacteria. *J. Proteome Res.* 20:27–37
19. Cournac A, Marbouty M, Mozziconacci J, Koszul R. 2016. Generation and analysis of chromosomal contact maps of yeast species. *Methods Mol. Biol.* 1361:227–45

20. Cournac A, Marie-Nelly H, Marbouty M, Koszul R, Mozziconacci J. 2012. Normalization of a chromosomal contact map. *BMC Genom.* 13:436
21. Dame RT, Rashid F-ZM, Grainger DC. 2020. Chromosome organization in bacteria: mechanistic insights into genome structure and function. *Nat. Rev. Genet.* 21(4):227–42
22. Dewachter L, Verstraeten N, Fauvart M, Michiels J. 2018. An integrative view of cell cycle control in *Escherichia coli*. *FEMS Microbiol. Rev.* 42(2):116–36
23. Dillon SC, Dorman CJ. 2010. Bacterial nucleoid-associated proteins, nucleoid structure and gene expression. *Nat. Rev. Microbiol.* 8(3):185–95
24. Dorman CJ. 2014. H-NS-like nucleoid-associated proteins, mobile genetic elements and horizontal gene transfer in bacteria. *Plasmid* 75:1–11
25. Duigou S, Boccard F. 2017. Long range chromosome organization in *Escherichia coli*: The position of the replication origin defines the non-structured regions and the Right and Left macrodomains. *PLOS Genet.* 13(5):e1006758
26. Dupaigne P, Tonthat NK, Espeli O, Whitfill T, Boccard F, Schumacher MA. 2012. Molecular basis for a protein-mediated DNA-bridging mechanism that functions in condensation of the *E. coli* chromosome. *Mol. Cell* 48(4):560–71
27. El Karoui M, Biaudet V, Schbath S, Gruss A. 1999. Characteristics of Chi distribution on different bacterial genomes. *Res. Microbiol.* 150(9–10):579–87
28. Espeli O, Borne R, Dupaigne P, Thiel A, Gigant E, et al. 2012. A MatP-divisome interaction coordinates chromosome segregation with cell division in *E. coli*. *EMBO J.* 31(14):3198–211
29. Espeli O, Mercier R, Boccard F. 2008. DNA dynamics vary according to macrodomain topography in the *E. coli* chromosome. *Mol. Microbiol.* 68(6):1418–27
30. Espinosa E, Paly E, Barre F-X. 2020. High-resolution whole-genome analysis of sister-chromatid contacts. *Mol. Cell* 79(5):857–69.e3
31. Fisher JK, Bourniquel A, Witz G, Weiner B, Prentiss M, Kleckner N. 2013. Four-dimensional imaging of *E. coli* nucleoid organization and dynamics in living cells. *Cell* 153(4):882–95
32. Fitzgerald S, Kary SC, Alshabib EY, MacKenzie KD, Stoebel DM, et al. 2020. Redefining the H-NS protein family: A diversity of specialized core and accessory forms exhibit hierarchical transcriptional network integration. *Nucleic Acids Res.* 48(18):10184–98
33. Gao F. 2015. Bacteria may have multiple replication origins. *Front. Microbiol.* 6:324
34. Gray WT, Govers SK, Xiang Y, Parry BR, Campos M, et al. 2019. Nucleoid size scaling and intracellular organization of translation across bacteria. *Cell* 177(6):1632–48.e20
35. Gruber S. 2018. SMC complexes sweeping through the chromosome: going with the flow and against the tide. *Curr. Opin. Microbiol.* 42:96–103
36. Gruber S, Veening JW, Bach J, Blettinger M, Bramkamp M, Errington J. 2014. Interlinked sister chromosomes arise in the absence of condensin during fast replication in *B. subtilis*. *Curr. Biol.* 24(3):293–98
37. Guilhas B, Walter J-C, Rech J, David G, Walliser NO, et al. 2020. ATP-driven separation of liquid phase condensates in bacteria. *Mol. Cell* 79(2):293–303.e4
38. Guo MS, Haakonsen DL, Zeng W, Schumacher MA, Laub MT. 2018. A bacterial chromosome structuring protein binds overtwisted DNA to stimulate type II topoisomerases and enable DNA replication. *Cell* 175(2):583–97.e23
39. Hardy CD, Cozzarelli NR. 2005. A genetic selection for supercoiling mutants of *Escherichia coli* reveals proteins implicated in chromosome structure. *Mol. Microbiol.* 57(6):1636–52
40. Harms A, Treuner-Lange A, Schumacher D, Sogaard-Andersen L. 2013. Tracking of chromosome and replisome dynamics in *Myxococcus xanthus* reveals a novel chromosome arrangement. *PLOS Genet.* 9(9):e1003802
41. Hassler M, Shaltiel IA, Haering CH. 2018. Towards a unified model of SMC complex function. *Curr. Biol.* 28(21):R1266–81
42. Higgins NP, Yang X, Fu Q, Roth JR. 1996. Surveying a supercoil domain by using the gamma delta resolution system in *Salmonella typhimurium*. *J. Bacteriol.* 178(10):2825–35
43. Hug LA, Baker BJ, Anantharaman K, Brown CT, Probst AJ, et al. 2016. A new view of the tree of life. *Nat. Microbiol.* 1:16048

44. Huisman O, Faelen M, Girard D, Jaffé A, Toussaint A, Rouvière-Yaniv J. 1989. Multiple defects in *Escherichia coli* mutants lacking HU protein. *J. Bacteriol.* 171(7):3704–12
45. Hyman AA, Weber CA, Jülicher F. 2014. Liquid-liquid phase separation in biology. *Annu. Rev. Cell Dev. Biol.* 30:39–58
46. Imakaev M, Fudenberg G, McCord RP, Naumova N, Goloborodko A, et al. 2012. Iterative correction of Hi-C data reveals hallmarks of chromosome organization. *Nat. Methods* 9(10):999–1003
47. Johnson RC, Bruist MF, Simon MI. 1986. Host protein requirements for in vitro site-specific DNA inversion. *Cell* 46(4):531–39
48. Joyeux M. 2015. Compaction of bacterial genomic DNA: clarifying the concepts. *J. Phys. Condens. Matter.* 27(38):383001
49. Jun S, Mulder B. 2006. Entropy-driven spatial organization of highly confined polymers: lessons for the bacterial chromosome. *PNAS* 103(33):12388–93
50. Junier I, Boccard F, Espeli O. 2014. Polymer modeling of the *E. coli* genome reveals the involvement of locus positioning and macrodomain structuring for the control of chromosome conformation and segregation. *Nucleic Acids Res.* 42(3):1461–73
51. Kahramanoglou C, Seshasayee ASN, Prieto AI, Ibberson D, Schmidt S, et al. 2011. Direct and indirect effects of H-NS and Fis on global gene expression control in *Escherichia coli*. *Nucleic Acids Res.* 39(6):2073–91
52. Kamar RI, Banigan EJ, Erbas A, Giuntoli RD, de la Cruz MO, et al. 2017. Facilitated dissociation of transcription factors from single DNA binding sites. *PNAS* 114(16):E3251–57
53. Kavenoff R, Bowen BC. 1976. Electron microscopy of membrane-free folded chromosomes from *Escherichia coli*. *Chromosoma* 59(2):89–101
54. Koch C, Kahmann R. 1986. Purification and properties of the *Escherichia coli* host factor required for inversion of the G segment in bacteriophage Mu. *J. Biol. Chem.* 261(33):15673–78
55. Kono N, Arakawa K, Tomita M. 2011. Comprehensive prediction of chromosome dimer resolution sites in bacterial genomes. *BMC Genomics* 12:19
56. Köppen A, Krobitsch S, Thoms B, Wackernagel W. 1995. Interaction with the recombination hot spot chi in vivo converts the RecBCD enzyme of *Escherichia coli* into a chi-independent recombinase by inactivation of the RecD subunit. *PNAS* 92(14):6249–53
57. Krasilnikov AS, Podtelezhnikov A, Vologodskii A, Mirkin SM. 1999. Large-scale effects of transcriptional DNA supercoiling in vivo. *J. Mol. Biol.* 292(5):1149–60
58. Krylov AS, Zasedateleva OA, Prokopenko DV, Rouviere-Yaniv J, Mirzabekov AD. 2001. Massive parallel analysis of the binding specificity of histone-like protein HU to single- and double-stranded DNA with generic oligodeoxyribonucleotide microchips. *Nucleic Acids Res.* 29(12):2654–60
59. Lal A, Dhar A, Trostel A, Kouzine F, Seshasayee ASN, Adhya S. 2016. Genome scale patterns of supercoiling in a bacterial chromosome. *Nat. Commun.* 7:11055
60. Le TB, Laub MT. 2016. Transcription rate and transcript length drive formation of chromosomal interaction domain boundaries. *EMBO J.* 35(14):1582–95
61. Le TBK, Imakaev MV, Mirny LA, Laub MT. 2013. High-resolution mapping of the spatial organization of a bacterial chromosome. *Science* 342(6159):731–34
62. Lee CM, Wang G, Pertsinidis A, Marians KJ. 2019. Topoisomerase III acts at the replication fork to remove precatenanes. *J. Bacteriol.* 201(7):e00563-18
63. Levy O, Ptacin JL, Pease PJ, Gore J, Eisen MB, et al. 2005. Identification of oligonucleotide sequences that direct the movement of the *Escherichia coli* FtsK translocase. *PNAS* 102(49):17618–23
64. Lioy VS, Cournac A, Marbouty M, Duigou S, Mozziconacci J, et al. 2018. Multiscale structuring of the *E. coli* chromosome by nucleoid-associated and condensin proteins. *Cell* 172(4):771–83.e18
65. Lioy VS, Junier I, Lagage V, Vallet I, Boccard F. 2020. Distinct activities of bacterial condensins for chromosome management in *Pseudomonas aeruginosa*. *Cell Rep.* 33:108344
66. Liu LF, Wang JC. 1987. Supercoiling of the DNA template during transcription. *PNAS* 84(20):7024–27
67. Livny J, Yamaichi Y, Waldor MK. 2007. Distribution of centromere-like parS sites in bacteria: insights from comparative genomics. *J. Bacteriol.* 189(23):8693–703
68. Luo H, Gao F. 2019. DoriC 10.0: an updated database of replication origins in prokaryotic genomes including chromosomes and plasmids. *Nucleic Acids Res.* 47(D1):D74–77

69. Mäkelä J, Sherratt DJ. 2020. Organization of the *Escherichia coli* chromosome by a MukBEF axial core. *Mol. Cell* 78(2):250–60.e5
70. Marbouty M, Baudry L, Cournac A, Koszul R. 2017. Scaffolding bacterial genomes and probing host-virus interactions in gut microbiome by proximity ligation (chromosome capture) assay. *Sci. Adv.* 3(2):e1602105
71. Marbouty M, Le Gall A, Cattoni DI, Cournac A, Koh A, et al. 2015. Condensin- and replication-mediated bacterial chromosome folding and origin condensation revealed by Hi-C and super-resolution imaging. *Mol. Cell* 59(4):588–602
72. Martínez-Antonio A, Janga SC, Thieffry D. 2008. Functional organisation of *Escherichia coli* transcriptional regulatory network. *J. Mol. Biol.* 381(1):238–47
73. Mercier R, Petit MA, Schbath S, Robin S, El Karoui M, et al. 2008. The MatP/matS site-specific system organizes the terminus region of the *E. coli* chromosome into a macrodomain. *Cell* 135(3):475–85
74. Moulin L, Rahmouni AR, Boccard F. 2005. Topological insulators inhibit diffusion of transcription-induced positive supercoils in the chromosome of *Escherichia coli*. *Mol. Microbiol.* 55(2):601–10
75. Mukherjee S, Seshadri R, Varghese NJ, Eloe-Fadrosh EA, Meier-Kolthoff JP, et al. 2017. 1,003 reference genomes of bacterial and archaeal isolates expand coverage of the tree of life. *Nat. Biotechnol.* 35(7):676–83
76. Murtin C, Engelhorn M, Geiselmann J, Boccard F. 1998. A quantitative UV laser footprinting analysis of the interaction of IHF with specific binding sites: re-evaluation of the effective concentration of IHF in the cell. *J. Mol. Biol.* 284(4):949–61
77. Nielsen HJ, Ottesen JR, Youngren B, Austin SJ, Hansen FG. 2006. The *Escherichia coli* chromosome is organized with the left and right chromosome arms in separate cell halves. *Mol. Microbiol.* 62(2):331–38
78. Niki H, Jaffe A, Imamura R, Ogura T, Hiraga S. 1991. The new gene *mukB* codes for a 177 kd protein with coiled-coil domains involved in chromosome partitioning of *E. coli*. *EMBO J.* 10(1):183–93
79. Niki H, Yamaichi Y, Hiraga S. 2000. Dynamic organization of chromosomal DNA in *Escherichia coli*. *Genes Dev.* 14(2):212–23
80. Nolivos S, Upton AL, Badrinarayanan A, Muller J, Zawadzka K, et al. 2016. MatP regulates the coordinated action of topoisomerase IV and MukBEF in chromosome segregation. *Nat. Commun.* 7:10466
81. Ozaki S, Jenal U, Katayama T. 2020. Novel divisome-associated protein spatially coupling the Z-ring with the chromosomal replication terminus in *Caulobacter crescentus*. *mBio* 11(2):e00487-20
82. Petrushenko ZM, She W, Rybenkov VV. 2011. A new family of bacterial condensins. *Mol. Microbiol.* 81(4):881–96
83. Pinson V, Takahashi M, Rouviere-Yaniv J. 1999. Differential binding of the *Escherichia coli* HU, homodimeric forms and heterodimeric form to linear, gapped and cruciform DNA. *J. Mol. Biol.* 287(3):485–97
84. Planchenault C, Pons MC, Schiavon C, Siguier P, Rech J, et al. 2020. Intracellular positioning systems limit the entropic eviction of secondary replicons toward the nucleoid edges in bacterial cells. *J. Mol. Biol.* 432(3):745–61
85. Prieto AI, Kahramanoglou C, Ali RM, Fraser GM, Seshasayee ASN, Luscombe NM. 2012. Genomic analysis of DNA binding and gene regulation by homologous nucleoid-associated proteins IHF and HU in *Escherichia coli* K12. *Nucleic Acids Res.* 40(8):3524–37
86. Qin L, Erkelens AM, Ben Bdira F, Dame RT. 2019. The architects of bacterial DNA bridges: a structurally and functionally conserved family of proteins. *Open Biol.* 9(12):190223
87. Rahmouni AR, Wells RD. 1992. Direct evidence for the effect of transcription on local DNA supercoiling in vivo. *J. Mol. Biol.* 223(1):131–44
88. Rajasekar KV, Baker R, Fisher GLM, Bolla JR, Mäkelä J, et al. 2019. Dynamic architecture of the *Escherichia coli* structural maintenance of chromosomes (SMC) complex, MukBEF. *Nucleic Acids Res.* 47(18):9696–707
89. Reyes-Lamothe R, Sherratt DJ. 2019. The bacterial cell cycle, chromosome inheritance and cell growth. *Nat. Rev. Microbiol.* 17(8):467–78
90. Ricci DP, Melfi MD, Lasker K, Dill DL, McAdams HH, Shapiro L. 2016. Cell cycle progression in *Caulobacter* requires a nucleoid-associated protein with high AT sequence recognition. *PNAS* 113(40):E5952–61

91. Rovinskiy N, Agbleke AA, Chesnokova O, Pang Z, Higgins NP. 2012. Rates of gyrase supercoiling and transcription elongation control supercoil density in a bacterial chromosome. *PLOS Genet*. 8(8):e1002845
92. Sánchez-Romero MA, Casadesús J. 2020. The bacterial epigenome. *Nat. Rev. Microbiol.* 18(1):7–20
93. Sayyed HE, Chat LL, Lebailly E, Vickridge E, Pages C, et al. 2016. Mapping topoisomerase IV binding and activity sites on the *E. coli* genome. *PLOS Genet*. 12(5):e1006025
94. Scheirer KE, Higgins NP. 2001. Transcription induces a supercoil domain barrier in bacteriophage Mu. *Biochimie* 83(2):155–59
95. Schmidt A, Kochanowski K, Vedelaar S, Ahrné E, Volkmer B, et al. 2016. The quantitative and condition-dependent *Escherichia coli* proteome. *Nat. Biotechnol.* 34(1):104–10
96. Schneider R, Lurz R, Lüder G, Tolksdorf C, Travers A, Muskhelishvili G. 2001. An architectural role of the *Escherichia coli* chromatin protein FIS in organising DNA. *Nucleic Acids Res*. 29(24):5107–14
97. Schneider R, Travers A, Muskhelishvili G. 1997. FIS modulates growth phase–dependent topological transitions of DNA in *Escherichia coli*. *Mol. Microbiol.* 26(3):519–30
98. Shen BA, Landick R. 2019. Transcription of bacterial chromatin. *J. Mol. Biol.* 431(20):4040–66
99. Shendruk TN, Bertrand M, de Haan HW, Harden JL, Slater GW. 2015. Simulating the entropic collapse of coarse-grained chromosomes. *Biophys J*. 108(4):810–20
100. Sinden RR, Pettijohn DE. 1981. Chromosomes in living *Escherichia coli* cells are segregated into domains of supercoiling. *PNAS* 78(1):224–28
101. Skoko D, Yoo D, Bai H, Schnurr B, Yan J, et al. 2006. Mechanism of chromosome compaction and looping by the *Escherichia coli* nucleoid protein Fis. *J. Mol. Biol.* 364(4):777–98
102. Staczek P, Higgins NP. 1998. Gyrase and Topo IV modulate chromosome domain size in vivo. *Mol. Microbiol.* 29(6):1435–48
103. Stein RA, Deng S, Higgins NP. 2005. Measuring chromosome dynamics on different time scales using resolvases with varying half-lives. *Mol. Microbiol.* 56(4):1049–61
104. Strom AR, Brangwynne CP. 2019. The liquid nucleome—phase transitions in the nucleus at a glance. *J. Cell Sci.* 132(22):jcs235093
105. Sutormin D, Rubanova N, Logacheva M, Ghilarov D, Severinov K. 2019. Single-nucleotide-resolution mapping of DNA gyrase cleavage sites across the *Escherichia coli* genome. *Nucleic Acids Res*. 47(3):1373–88
106. Taylor JA, Panis G, Viollier PH, Marczynski GT. 2017. A novel nucleoid-associated protein coordinates chromosome replication and chromosome partition. *Nucleic Acids Res*. 45(15):8916–29
107. Thiel A, Valens M, Vallet-Gely I, Espeli O, Boccard F. 2012. Long-range chromosome organization in *E. coli*: a site-specific system isolates the Ter macrodomain. *PLOS Genet*. 8(4):e1002672
108. Tonthat NK, Arold ST, Pickering BF, Van Dyke MW, Liang S, et al. 2011. Molecular mechanism by which the nucleoid occlusion factor, SlmA, keeps cytokinesis in check. *EMBO J*. 30(1):154–64
109. Touchon M, Rocha EPC. 2016. Coevolution of the organization and structure of prokaryotic genomes. *Cold Spring Harb. Perspect. Biol.* 8(1):a018168
110. Touzain F, Petit M-A, Schbath S, Karoui ME. 2011. DNA motifs that sculpt the bacterial chromosome. *Nat. Rev. Microbiol.* 9(1):15–26
111. Tran NT, Laub MT, Le TBK. 2017. SMC progressively aligns chromosomal arms in *Caulobacter crescentus* but is antagonized by convergent transcription. *Cell Rep*. 20(9):2057–71
112. Trussart M, Yus E, Martinez S, Baù D, Tahara YO, et al. 2017. Defined chromosome structure in the genome-reduced bacterium *Mycoplasma pneumoniae*. *Nat. Commun.* 8(1):14665
113. Umbarger MA, Toro E, Wright MA, Porreca GJ, Bau D, et al. 2011. The three-dimensional architecture of a bacterial genome and its alteration by genetic perturbation. *Mol. Cell* 44(2):252–64
114. Valens M, Penaud S, Rossignol M, Cornet F, Boccard F. 2004. Macrodomain organization of the *Escherichia coli* chromosome. *EMBO J*. 23(21):4330–41
115. Valens M, Thiel A, Boccard F. 2016. The MaoP/*maoS* site-specific system organizes the Ori region of the *E. coli* chromosome into a macrodomain. *PLOS Genet*. 12(9):e1006309
116. Vallet-Gely I, Boccard F. 2013. Chromosomal organization and segregation in *Pseudomonas aeruginosa*. *PLOS Genet*. 9(5):e1003492
117. Vazquez Nunez R, Ruiz Avila LB, Gruber S. 2019. Transient DNA occupancy of the SMC interarm space in prokaryotic condensin. *Mol. Cell* 75(2):209–23.e6

118. Verma SC, Qian Z, Adhya SL. 2019. Architecture of the *Escherichia coli* nucleoid. *PLOS Genet*. 15(12):e1008456
119. Viollier PH, Thanbichler M, McGrath PT, West L, Meewan M, et al. 2004. Rapid and sequential movement of individual chromosomal loci to specific subcellular locations during bacterial DNA replication. *PNAS* 101(25):9257–62
120. Vora T, Hottes AK, Tavazoie S. 2009. Protein occupancy landscape of a bacterial genome. *Mol. Cell* 35(2):247–53
121. Wang S, Cosstick R, Gardner JF, Gumport RI. 1995. The specific binding of *Escherichia coli* integration host factor involves both major and minor grooves of DNA. *Biochemistry* 34(40):13082–90
122. Wang W, Li GW, Chen C, Xie XS, Zhuang X. 2011. Chromosome organization by a nucleoid-associated protein in live bacteria. *Science* 333(6048):1445–49
123. Wang X, Brandão HB, Le TBK, Laub MT, Rudner DZ. 2017. *Bacillus subtilis* SMC complexes juxtapose chromosome arms as they travel from origin to terminus. *Science* 355(6324):524–27
124. Wang X, Le TBK, Lajoie BR, Dekker J, Laub MT, Rudner DZ. 2015. Condensin promotes the juxtaposition of DNA flanking its loading site in *Bacillus subtilis*. *Genes Dev*. 29(15):1661–75
125. Wang X, Liu X, Possoz C, Sherratt DJ. 2006. The two *Escherichia coli* chromosome arms locate to separate cell halves. *Genes Dev*. 20(13):1727–31
126. Wang X, Montero Llopis P, Rudner DZ. 2014. *Bacillus subtilis* chromosome organization oscillates between two distinct patterns. *PNAS* 111(35):12877–82
127. Wang X, Tang OW, Riley EP, Rudner DZ. 2014. The SMC condensin complex is required for origin segregation in *Bacillus subtilis*. *Curr. Biol.* 24(3):287–92
128. Weber PM, Moessel F, Paredes GF, Viehboeck T, Vischer NOE, Bulgheresi S. 2019. A bidimensional segregation mode maintains symbiont chromosome orientation toward its host. *Curr. Biol.* 29(18):3018–28.e4
129. Wilhelm L, Bürmann F, Minnen A, Shin H-C, Toseland CP, et al. 2015. SMC condensin entraps chromosomal DNA by an ATP hydrolysis dependent loading mechanism in *Bacillus subtilis*. *eLife* 4:e06659
130. Worcel A, Burgi E. 1972. On the structure of the folded chromosome of *Escherichia coli*. *J. Mol. Biol.* 71(2):127–47
131. Wu F, Japaridze A, Zheng X, Wiktor J, Kerssemakers JWJ, Dekker C. 2019. Direct imaging of the circular chromosome in a live bacterium. *Nat. Commun.* 10(1):2194
132. Wu F, Swain P, Kuijpers L, Zheng X, Felter K, et al. 2019. Cell boundary confinement sets the size and position of the *E. coli* chromosome. *Curr. Biol.* 29(13):2131–44.e4
133. Wu LJ, Ishikawa S, Kawai Y, Oshima T, Ogasawara N, Errington J. 2009. Noc protein binds to specific DNA sequences to coordinate cell division with chromosome segregation. *EMBO J.* 28(13):1940–52
134. Yatskevich S, Rhodes J, Nasmyth K. 2019. Organization of chromosomal DNA by SMC complexes. *Annu. Rev. Genet.* 53:445–82
135. Youngren B, Nielsen HJ, Jun S, Austin S. 2014. The multifork *Escherichia coli* chromosome is a self-duplicating and self-segregating thermodynamic ring polymer. *Genes Dev*. 28(1):71–84
136. Zawadzki P, Stracy M, Ginda K, Zawadzka K, Lesterlin C, et al. 2015. The localization and action of topoisomerase IV in *Escherichia coli* chromosome segregation is coordinated by the SMC complex, MukBEF. *Cell Rep*. 13(11):2587–96
137. Zechiedrich EL, Khodursky AB, Cozzarelli NR. 1997. Topoisomerase IV, not gyrase, decatenates products of site-specific recombination in *Escherichia coli*. *Genes Dev*. 11(19):2580–92